Vol. 508: 67–85, 2014
doi: 10.3354/meps10841

MARINE ECOLOGY PROGRESS SERIES
Mar Ecol Prog Ser

Published August 4

Microbial distribution in different spatial positions within the walls of a black sulfide hydrothermal chimney

Jiangtao Li[1], Huaiyang Zhou[1,*], Jiasong Fang[1,2,*], Yannan Sun[1], Shamik Dasgupta[1]

[1]State Key Laboratory of Marine Geology, Tongji University, Shanghai 200092, PR China
[2]Department of Natural Sciences, Hawaii Pacific University, Kaneohe, Hawaii 96744, USA

ABSTRACT: Deep-sea hydrothermal chimneys encompass diverse niches for different microbial communities with steep environmental gradients. An active sulfide hydrothermal structure was recovered from the Dudley site of the Main Endeavour Field in the Juan de Fuca Ridge. Subsamples were taken from different spatial positions within the chimney wall and analyzed for mineral composition and microbial biomass and community structure to illustrate the characteristics of microbial distribution and environmental constraints. Mineral analysis showed that the chimney was mainly composed of various Fe-, Zn-, and Cu-rich sulfides, with mineral composition and abundance varying with spatial position. Microbial populations in the chimney predominantly consisted of archaeal members affiliated with the deep-sea hydrothermal vent *Euryarchaeota* group, *Thermococcales*, and *Desulfurococcales*, as well as bacterial members of the *Gamma-*, *Epsilon-*, and *Deltaproteobacteria*. Microbial biomass and composition shifted dramatically and formed different microbial zones within the chimney walls, from predominantly mesophilic, sulfur-oxidizing bacterial communities at the outer surfaces to thermophilic or hyperthermophilic, archaeal sulfur-reducers in the inner layers of the chimney. Based on microbial physiological characteristics and their distribution profiles, we inferred that temperature, fluid geochemistry, and organic compounds probably play an important role in selecting for and sustaining microbial communities. Furthermore, *in situ* temperature regimes within the chimney walls were roughly estimated based on the temperatures supporting the growth of the dominant microbial groups.

KEY WORDS: Deep-sea · Hydrothermal vents · Chimney · Microbial distribution · Temperature gradient

INTRODUCTION

In the past 3 decades, numerous microbiological surveys of deep-sea hydrothermal vents have been carried out utilizing culture-dependent and -independent approaches because of the extreme environmental conditions and unique microbial populations of the vents (Hoek et al. 2003, Miroshnichenko et al. 2003, Nakagawa et al. 2005c, McCliment et al. 2006, Takai et al. 2006, Wang et al. 2009, Zhou et al. 2009, Nunoura et al. 2010). In general, microbial diversity and distribution within different hydrothermal vents are consistent with local environmental parameters (Emerson & Moyer 2002, Takai et al. 2004, Brazelton et al. 2006, Perner et al. 2007), which can be attributed to the geochemical and thermodynamic constraints on primary producers (McCollom & Shock 1997, McCollom 2000).

*Corresponding authors: zhouhy@tongji.edu.cn; jfang@hpu.edu

One of the most fascinating features of the sulfide structures is the steep temperature and geochemical gradients at very small spatial scales. The shift from hot (245~350°C), reduced, and metal-enriched hydrothermal fluids to cold (2~15°C), oxygenated, and sulfate-rich surrounding seawater occurs within decimeters across the chimney walls. Different mineral assemblages with varying pore spaces, cracks, and fissures make chimney walls heterogeneous. Diverse niches are formed within vent chimneys with enormous physical and geochemical differences in the mixing processes between hydrothermal fluids and the circulating seawater, and these niches support different microbial populations (Tivey & McDuff 1990, Kelley et al. 2002, Perner et al. 2007). Although numerous studies investigating spatial distributions of microbes in deep-sea hydrothermal environments have been published (Nakagawa et al. 2005c, Brazelton et al. 2006, Opatkiewicz et al. 2009, Nunoura et al. 2010, Li et al. 2012), relatively limited analyses have been done so far to illustrate the microbial characteristics in different spatial positions across a single structure and to explore the relationship between environmental conditions and microbial components within the walls of active chimneys. An early study by Takai et al. (2001) revealed archaeal distribution in a black smoker and showed that archaeal communities varied in different microhabitats. Subsequently, Schrenk et al. (2003) examined an active chimney from the Edifice Rex project and found variations in the abundance and diversity of archaea from the exterior to the interior walls of the chimney. More recently, Kormas et al. (2006) attempted to correlate microbial distribution with environmental regimes in distinct mineral layers of a white smoker, on the basis of 16S rRNA gene cloning and mineralogical analysis. Nevertheless, microbial distribution in chimney walls and potential constraints of microenvironments across a single structure remain unclear.

In 2005, an active sulfide black chimney was collected by RV 'Atlantis/Alvin' from the Dudley hydrothermal site of the Main Endeavour Field during a China–USA joint dive cruise to Juan de Fuca Ridge. The goal of this study was to describe and compare microbial communities in different zones within this chimney wall, and to explore the relationship between microbial distributions and possible environmental constraints. To achieve these goals, subsamples of the Dudley chimney walls were taken; based on their positions, these were of different porosities, and mineral assemblages.

MATERIALS AND METHODS

Site description, sample collection, and subsampling procedure

The Main Endeavour Field (47° 57′ N, 129° 05′ W), at a water depth of 2200 m, is 1 of the 5 hydrothermal vent fields within the Endeavour Segment of the Juan de Fuca Ridge. A number of large, steep-sided active and inactive hydrothermal sulfide structures are located in the active faults and fissures (Fig. 1) (Delaney et al. 1992, Butterfield et al. 1994). The sulfide black smoker was collected at the Dudley site by DSV 'Alvin' (Dive No. 4132) in 2005. The chimney was actively venting hydrothermal fluids, and the maximum measured temperature of the fluid exiting from the orifice of the chimney was 330°C. The collected structure was about 25 cm long and 12 cm wide with a central irregular conduit varying in diameter from ca. 0.5 to 5 cm (Fig. 2). The chimney was stored at −20°C immediately after shipboard recovery and then preserved in dry ice during transportation to our lab. Subsamples for further analysis were taken from different locations along a horizontal transect across the chimney wall from the exterior surface to the interior fluid conduit; these varied in porosity, and mineralogy. When the chimney was cut along the horizontal transect, 2 different fluid conduits were revealed. Conduit P (see Fig. 2) was still open, venting high temperature hydrothermal fluids, whereas conduit Q (Fig. 2) was already closed and was filled nearly completely by minerals. During subsampling of the chimney, all tools including tweezers, toothdrills, and mortar were sterilized, and operators wore gloves and facemasks to eliminate potential contamination. In total, 10 subsamples were taken from the chimney as shown in Fig. 2: 1 subsample (P0) from the central irregular conduit, 2 subsamples (P3 and Q3) from the innermost part, 2 (P1, Q1) from the exterior and outermost walls, and the rest from the middle layers of the chimney walls (P2 and Q2 from outer-middle; P4, P5, and P6 from inner-middle). These subsamples were split into several parts for different analyses including mineralogy, elemental composition, DNA extraction, and ultrastructure observation.

Mineralogical analysis

All subsamples (ca. 1 g of each) for mineralogical and chemical analyses were dried at 50°C and then ground using a mortar and pestle. X-ray diffraction

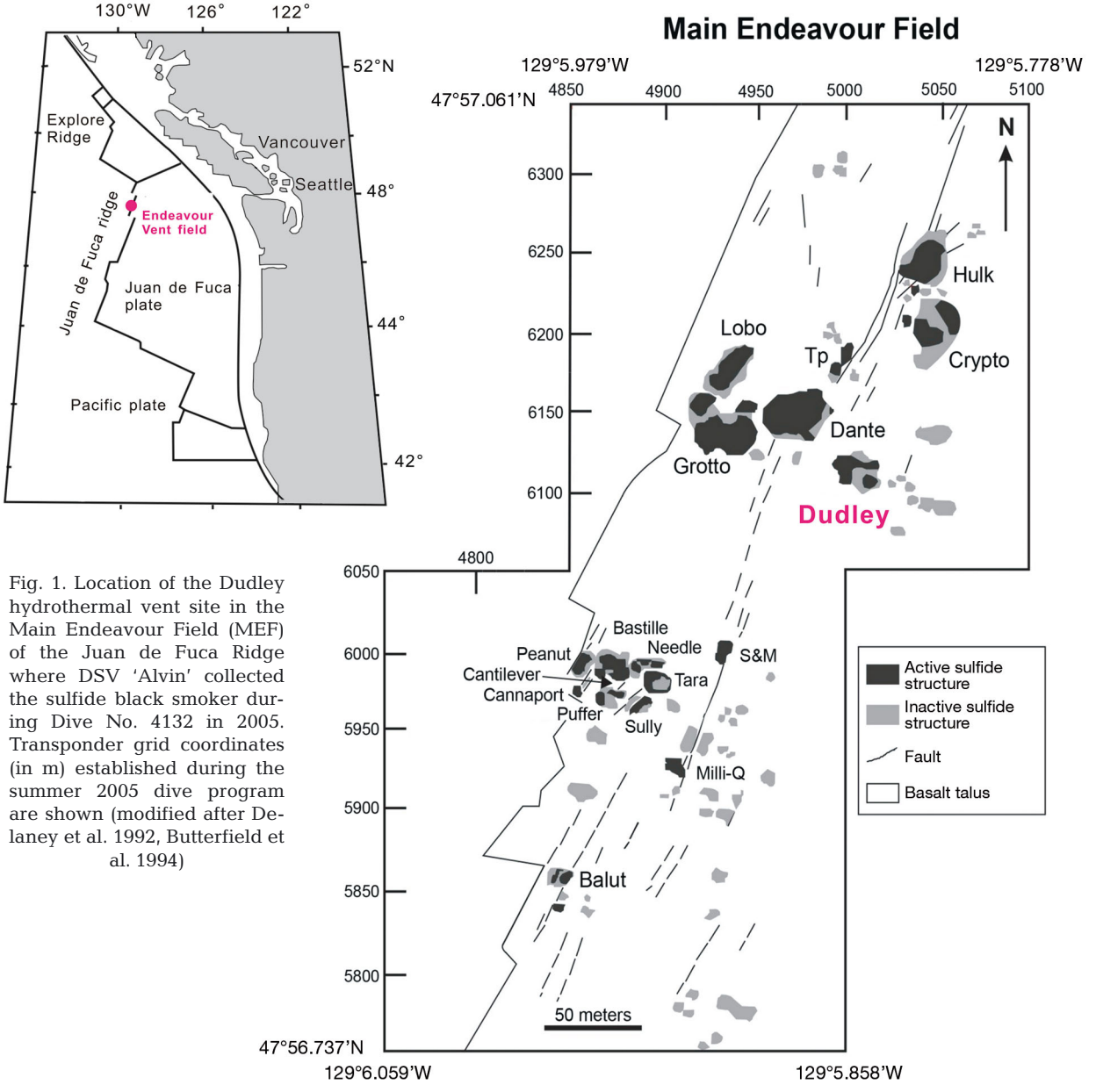

Fig. 1. Location of the Dudley hydrothermal vent site in the Main Endeavour Field (MEF) of the Juan de Fuca Ridge where DSV 'Alvin' collected the sulfide black smoker during Dive No. 4132 in 2005. Transponder grid coordinates (in m) established during the summer 2005 dive program are shown (modified after Delaney et al. 1992, Butterfield et al. 1994)

(XRD) pattern analysis was then performed by a Rint 2000 X-ray diffractometer (Rigaku) using Cu Kα radiation at 40 kV and 30 mA. Diffraction angles (referred to as 2θ) corresponding to the atomic structure unique to each mineral were measured.

Scanning electron microscopy

Samples were observed using an FEI Quant 400 environmental scanning electron microscope (SEM). Gold coating on surfaces was not required for wet samples using environmental SEM, which avoided influence of pretreatment on spectral analysis. Micro-area chemical composition of mineral surfaces was analyzed on a Genesis energy dispersive spectrometer (EDAX).

DNA extraction, amplification, and cloning

DNA was extracted following the sodium dodecyl sulfate (SDS)-based extraction method with some modifications (Zhou et al. 1996). About 5 g of each sample were mixed with 13.5 ml of DNA extraction buffer (100 mM Tris-HCl, 100 mM sodium EDTA,

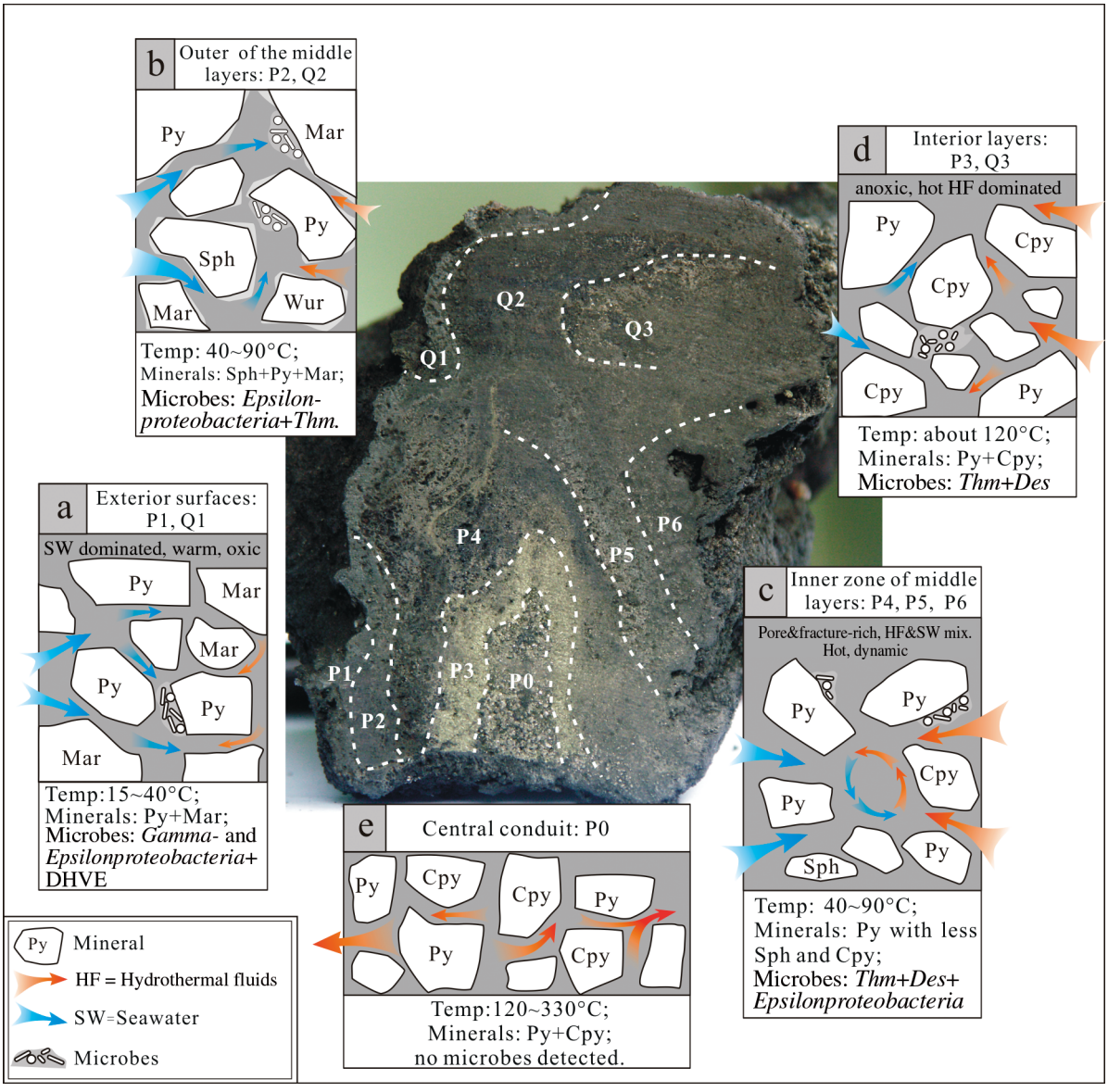

Fig. 2. Subsampling positions along the cross-section of the sulfide chimney and schematics providing information on inferred temperature, mineral composition, microbial populations, and possible environmental characteristics in different layers in the chimney walls (scale bar = 5 cm). Two conduits were distinguished: conduit P actively vented hydrothermal fluids of ~330°C, while Q was inactive and was filled with various minerals. (a) Exterior surface. (b) Outer zone of the middle layers, which was affected by seawater (SW) and hydrothermal fluids (HF) by means of thermal conductivity. (c) Inner zone of the middle layers. Pores and fractures were abundant, causing intensive mixing of SW and HF. Generally, the middle layer (outer and inner parts) is a hot (40–90°C), heterogeneous, and dynamic environment where both bacteria and archaea bloom. Hyperthermophilic heterotrophs dominated here as a result of the abundance of organic substrates. (d) Inner layer close to the central conduits. This layer is a very hot (90–121°C), anoxic, and reductive environment mainly affected by HF. (e) Active central conduit. This zone is too hot (300–330°C) to sustain microbes. Py: pyrite; Mar: marcasite; Sph: sphalerite; Wur: wurtzite; Cpy: chalcopyrite; *Thm*: *Thermococcales*; *Des*: *Desulfurococcales*; DHVE: deep-sea hydrothermal vent *Euryarchaeota*

100 mM sodium phosphate, 1.5 M NaCl, 1% CTAB) and 100 µl of Proteinase K (10 mg ml^{-1}, Sigma) in tubes by horizontal shaking at 225 rpm (30 min at 37°C). After shaking, 1.5 ml of 20% (w/v) SDS was added, and samples were incubated in a 65°C water bath for 2 h. The supernatants were collected after centrifugation at 6000 × *g* (10 min) and transferred into 50 ml centrifuge tubes. The supernatants were then mixed with an equal volume of chloroform: isoamyl alcohol (24:1, v/v). The aqueous phase was recovered by centrifugation (16 000 × *g*) and precipitated with 0.6 volume of isopropanol for about 1 h.

Crude nucleic acids were obtained by centrifugation at 16 000 × *g* (20 min at room temperature), washed with 70% ethanol, and resuspended in sterile deionized water. The crude nucleic acids were purified with a cycle-pure kit (Omega).

16S rRNA genes were amplified from extracted DNA by using *Ex Taq* polymerase with 10× buffer (Takara Bio). Bacterial 16S rDNA was amplified using the primers Eubac27f (5′-AGA GTT TGA TCC TGG CTC AG-3′) and Eubac1492r (5′-GGT TAC CTT GTT ACG ACT T-3′), and the primers Arch21f (5′-TTC CGG TTG ATC CYG CCG GA-3′) and Arch958r (5′-YCC GGC GTT GAM TCC AAT T-3′) were used for archaea with products of 1500 and 900 bp, respectively. Amplification conditions were as follows: an initial denaturation step of 94°C for 4 min followed by 30 cycles of denaturation at 94°C for 60 s, annealing at 55°C for 45 s, and extension at 72°C for 60 s, and a final extension step of 72°C for 10 min. The PCR products were purified with a gel-extraction kit (Omega) following the manufacturer's instructions. Purified PCR products were cloned into pMD18-T vectors (Takara) and transformed to competent *Escherichia coli* DH5α cells (Takara). Inserts of the correct size were screened with the vector-specific primers M13f (5′-GTA AAA CGA CGG CCA G-3′) and M13r (5′-CAG GAA ACA GCT ATG AC-3′). Clones containing target 16S rDNA were subjected to restriction fragment length polymorphism (RFLP) analyses, which were performed for every clone library independently. Inserted fragments were digested with the restriction enzymes *Rsa*I and *Msp*I (Takara) according to the manufacturer's instructions. Digested DNA fragments were then separated on a 3% (w/v) agarose gel. Representative archaeal and bacterial clones with unique RFLP banding patterns were chosen for sequencing.

Sequencing and phylogenetic analysis

The representative clones chosen from each clone library after the RFLP analysis were sequenced with an ABI PRISM 3730XL automated sequencer with T-vector universal primers. For the sequences of the 16S rRNA gene, chimeric sequences were checked using Bellerophon (3.0) at http://greengenes.lbl.gov (Huber et al. 2004, DeSantis et al. 2006).The program DOTUR was then used to determine the operational taxonomic units (OTUs) or phylotypes for all archaeal and bacterial sequences, respectively, using a 97% similarity cutoff (Schloss & Handelsman 2005). Sequences of phylotypes were submitted to the Advanced BLAST search program (available through the National Center for Biotechnology Information) to find closely related sequences in the GenBank and EMBL databases for phylogenetic analysis. All phylotypes and their relatives were aligned using ClustalX 2.0.1 (Larkin et al. 2007). Phylogenetic trees were constructed by neighbor-joining (NJ) using Mega 5.0 (Tamura et al. 2011). Bootstrap analysis was used to provide confidence estimates of tree topologies.

Quantification of the 16S rRNA gene

The microbial 16S rRNA gene was quantified by fluorescence quantitative real-time PCR. The inserted DNA fragments of clones P3-a27 (from the archaeal 16S rRNA gene library) and P3-b36 (from the bacterial 16S rRNA gene library) were amplified and purified to generate standard DNAs for archaeal and bacterial 16S rRNA gene quantification using the primers Arch344f and Arch519r (Bano et al. 2004) and Eubac341f and Eubac518r (Dilly et al. 2004), respectively. The products were quantified and 10-fold dilutions ranging from 10^7 to 10^2 copies were used as the quantification standards. Amplifications were performed on the 7500 real-time PCR system (Applied Biosystems) in a 20 µl reaction mixture that consisted of 1 µl template DNA (1 to 10 ng), 0.15 µM of each primer, and 10 µl of Power SYBR green PCR master mix (Applied Biosystems) with ROX and SYBR green I. Negative control and gel electrophoresis after each quantitative PCR experiment were also carried out. For the negative control, only 1 primer dimer with a length of about 100 bp occurred, while for the samples, just 1 single and bright band (about 200 bp) appeared. Melting curve analysis was performed after amplification, and the cycle threshold was set automatically using System 7500 software (1.3). The copy number of the 16S rRNA gene was calculated as the average of triplicate samples (Nunoura & Takai 2009). Bacterial and archaeal density could be calculated based on the assumption that every cell contained 3.45 or 1.00 16S rRNA gene copies on average, respectively (see Fig. 3) (Lee et al. 2009).

Statistical analysis

To compare the differences among the microbial communities inhabiting different parts of the sulfide chimney, we applied principal component analysis (PCA) to all archaeal and bacterial 16S rRNA gene li-

braries using the online UniFrac program (http://bmf2.colorado.edu/unifrac/index.psp) (Lozupone & Knight 2005). To perform PCA, the phylogenetic tree of all archaeal and bacterial phylotypes was constructed with the NJ method using the software Phylip 3.65, and the abundance weights (shown in Tables S1 & S2 in the Supplement at www.int-res.com/articles/suppl/m508p067_supp.pdf) of all phylotypes within their own libraries were also considered.

Nucleotide sequence accession numbers

Bacterial and archaeal sequences were deposited in GenBank under the following accession numbers: JQ072906–JQ073012 and JQ073013–JQ073047, respectively.

RESULTS

Mineralogy and SEM observations

XRD analysis showed that the chimney was mainly composed of various Fe-, Zn-, and Cu-rich sulfide minerals such as pyrite (FeS_2), marcasite (FeS_2), wurtzite-sphalerite (ZnS), and chalcopyrite ($CuFeS_2$; Table 1). It was clear that the minerals varied in composition and abundance with their positions in the chimney. The exterior rims encompassed the outer part (ca. 0.8~1.2 cm) of the chimney wall and mainly consisted of marcasite and pyrite (P1: 28.4 and 41.7%; Q1: 39.3 and 41.5%), with minor amounts of wurtzite, sphalerite, and barite ($BaSO_4$). In contrast, the central conduit (sample P0) was characterized by high abundance of chalcopyrite (49.4%) and pyrite (34.8%), with smaller amounts of wurtzite and sphalerite (~5% each). The interior layers, including sample Q3, which was at one time an internal conduit but was already filled by minerals at the time of collection, and sample P3, located adjacent to the active central channel, were commonly dominated by pyrite (>70%), with minor amounts of sphalerite and chalcopyrite. The middle layers (P2, P4, P5, P6, and Q2) contained variable amounts of pyrite, marcasite, wurtzite/sphalerite, and chalcopyrite. Samples P2 and Q2, taken from the outer zone of the middle layers, showed similar mineral composition including similar proportions of pyrite, sphalerite, and marcasite, with minor amounts of wurtzite and chalcopyrite. Samples P4, P5, and P6, all from the inner part of the middle layers, contained more pores and fissures (shown in Fig. 2). Pyrite was the dominant mineral phase (nearly 70%); other minerals such as marcasite, chalcopyrite, and Zn-Fe sulfides were also present. Other minor minerals found include elemental sulfur, barite, and amorphous silica.

Results of SEM observation were consistent with the result of XRD analysis. Perfect crystals of sulfide minerals such as chalcopyrite, pyrite, marcasite, wurtzite, and sphalerite were observed (shown in Fig. S1 in the Supplement). Amorphous silica was precipitated and coated on the surfaces of the minerals or in the spaces between them (Fig. S1g). In addition, some rod- and filament-like structures resembling microbes were also observed (e.g. P4) which were heavily covered with amorphous silica (Fig. S1d,e). This was confirmed by energy-dispersive spectrophotometry (data not shown).

Microbial biomass estimates

DNA was extracted successfully from 9 samples except the one from the open central conduit, P0. It is possible that the central channel was uninhabitable

Table 1. Mineral composition (%) of the hydrothermal sulfide chimney collected from the Dudley site of the Main Endeavour Field in the Juan de Fuca Ridge. See Fig. 2 for subsampling positions in the chimney. –: not detected

Position	Pyrite	Sphalerite	Chalcopyrite	Wurtzite	Marcasite	Fe-sulfides	Barite	Sulfur	Other
P1	41.7	4.30	3.20	6.3	28.4	4.6	5.5	–	6.0
P2	21.8	23.5	6.20	13.0	20.7	–	–	2.0	13.0
P3	98.2	–	–	–	–	–	–	–	–
P0	34.8	5.20	49.4	4.60	–	–	–	–	6.0
P4	70.0	14.8	8.00	–	–	–	–	–	7.2
P5	64.8	–	5.50	4.50	21.2	–	–	–	4.0
P6	71.2	5.80	–	–	17.0	–	–	–	6.0
Q1	41.5	4.20	2.20	5.80	39.3	–	–	–	7.0
Q2	26.5	38.2	3.50	4.20	17.6	–	–	–	10
Q3	71.5	5.30	14.2	–	–	–	–	–	9.0

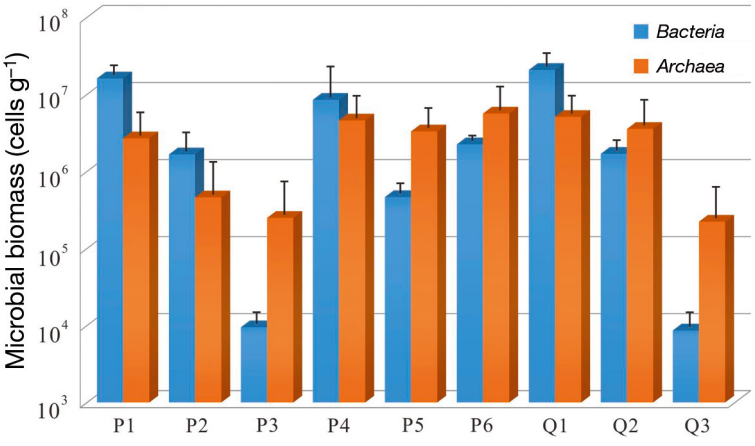

Fig. 3. Estimation of archaeal and bacterial biomass in different parts of the Dudley hydrothermal sulfide chimney. The error bars are SD, and *x*-axis indicates subsampling position. We determined copy numbers of the 16S rRNA gene and then calculated microbial density based on the assumption that every cell contained respectively 3.45 or 1.00 16S rRNA gene copies on average (Lee et al. 2009). See Fig. 2 for subsampling positions in the chimney

because the temperature was likely too high for microbes to survive. The small subunit 16S rRNA gene was quantified and converted to cell density by assuming an average 16S rRNA gene copy number of 3.45 and 1.00 per cell for bacteria and archaea, respectively (Lee et al. 2009). These 2 values were derived from average copy numbers of pure cultures, which were closely related to our phylotypes. In general, bacterial abundance showed greater variations than archaeal abundance. The exterior layers (P1 and Q1) contained the greatest number of bacterial cells (1.61×10^7 and 2.07×10^7 cells g^{-1} of sample, respectively), whereas the interior layers (P3 and Q3) had nearly 4 orders of magnitude lower cell abundance (9.46×10^3 and 8.60×10^3 cells g^{-1}, respectively). In the middle layers, bacterial cell density varied indistinctively, with an average of about 10^5~10^6 cells g^{-1} of sample. Although the distribution trend of archaeal biomass was similar to that of bacteria, cell numbers were less varied, ranging from 10^5 to 10^6 cells g^{-1}. The innermost layers (P3 and Q3) contained the lowest amounts of archaeal cells, about 2.49×10^5 to 2.22×10^5 cells g^{-1}, whereas the amounts in other positions (exterior surfaces and middle layers) fluctuated only slightly (approximately 10^6 cells g^{-1}). Generally, bacterial and archaeal biomass tended to increase gradually from the inner layers to the outer layers, except in sample P4 from the middle layer. As shown in Fig. 3, cell numbers detected in sample P4 reached 8.49×10^6 and 4.57×10^6 cells g^{-1} for bacteria and archaea, respectively, much higher than other samples collected from the middle layers. Although a potential methodological bias in calculating PCR-based cell numbers exists (Lloyd et al. 2013), these values are considered reasonable and consistent with several previous studies (e.g. Harmsen et al. 1997, Schrenk et al. 2003).

Archaeal phylotypes

Phylogenetic positions of each archaeal phylotype are shown in Figs. 4 & 5 and Table S1. These archaeal phylotypes were assigned to the following groups: *Desulfurococcales*, *Thermococcales*, *Thermoproteales*, *Archaeoglobales*, marine group I (MGI; Martin-Cuadrado et al. 2008), deep-sea hydrothermal vent *Euryarchaeota* (DHVE; Takai & Horikoshi 1999), which includes the subgroups DHVE1 (Nunoura et al. 2010), DHVE2 (Reysenbach et al. 2006, Nunoura & Takai 2009), DHVE9 (Pagé et al. 2004), DHVE10, DHVE11, and Korarchaeota (Takai & Sako 1999, Ehrhardt et al. 2007). In addition, there was 1 phylotype belonging to the unclassified *Crenarchaeota* (UC).

Phylotypes assigned to the *Desulfurococcales* group were detected commonly in 9 samples, although their proportions were minor in the exterior layer samples (P1 and Q1) and the outer zone of the middle layer (sample P2; Fig. 4a, Table S1). These phylotypes were clustered with environmental sequences detected at hydrothermal vents located in the Lau Basin, Japan Suiyo Seamount, Okinawa Trough, Mariana Trough, Mid-Atlantic Ridge, East Pacific Rise 9° N, Clam Bed Field, and the Central Indian Ridge (Fig. 5) (Ehrhardt et al. 2007, Wang et al. 2009). *Desulfurococcales* phylotypes in our study showed high similarity (>94 %) to pure cultures (data are partly shown in Fig. 5) of *Staphylothermus hellenicus*, *Geogemma indica*, *Hyperthermus butylicus*, *Aeropyrum premix*, *Thermogladius cellulolyticus*, *Desulfurococcus mucosus*, and others which are generally hyperthermophiles with optimum temperatures supporting growth (hereafter termed 'growth temperatures') above 90°C (Sako et al. 1996, Blöchl et al. 1997).

Phylotypes representing members of the *Thermococcales* group were also found in samples from the exterior walls to internal layers of the chimney (Fig. 4a, Table S1). They dominated the middle and inner chimney layers with abundances greater than 50 %. Even the outer wall samples P1 and Q1 contained nearly 30 % *Thermococcales* phylotypes in

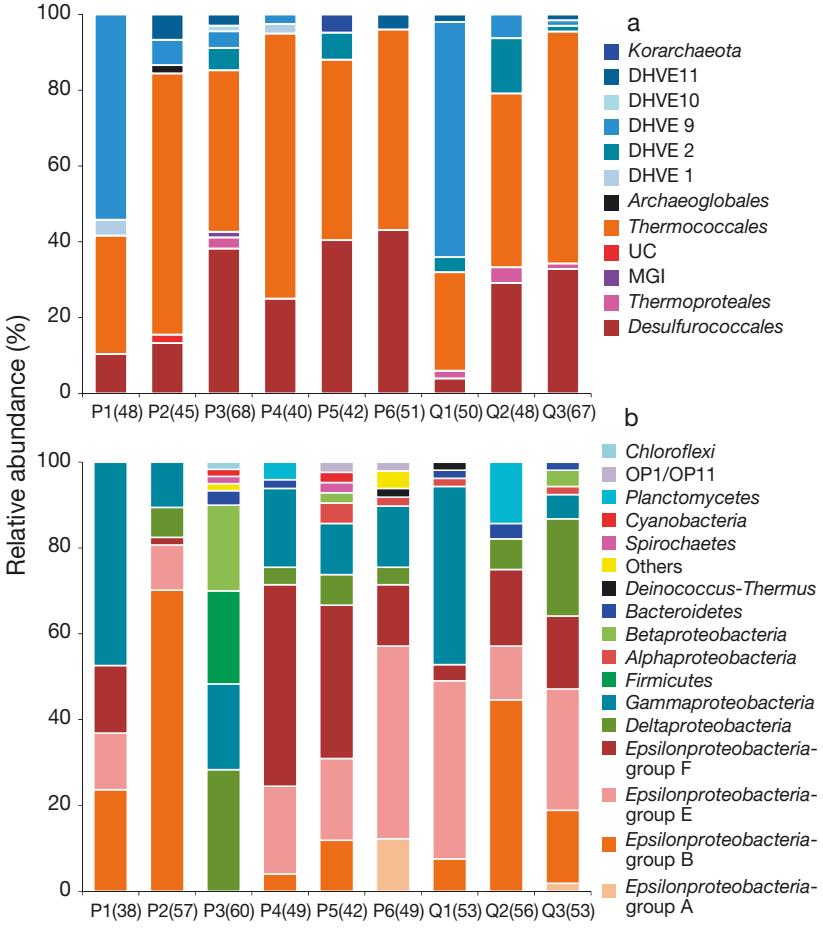

Fig. 4. Composition of the (a) archaeal and (b) bacterial microbial communities based on 16S rRNA gene clone libraries constructed from each subsample (*x*-axis) of the sulfide chimney. The relative abundances of the detected clones are shown. The numbers in parentheses indicate the total numbers of clones analyzed at each position. See Fig. 2 for subsampling positions in the chimney. DHVE: deep-sea hydrothermal vent *Euryarchaeota*, UC: unclassified *Crenarchaeota*, MGI: marine group I

their archaeal libraries. Environmental sequences and cultivated isolates highly similar to our phylotypes have been recovered exclusively from hydrothermal vents or other high-temperature environments (Huber et al. 2006, Nakagawa et al. 2006). Although some species are capable of formate oxidation or carboxydotrophy coupled with H_2 production, members of the genus *Thermococcus* are generally considered to be hyperthermophilic obligate anaerobes with a fermentative metabolism utilizing complex carbon sources (Ehrhardt et al. 2007).

DHVE clones were divided into 5 different subgroups, including 3 of the 9 groups existing prior to this study (DHVE 1, DHVE 2, DHVE 9) and the 2 newly assigned groups in this study (DHVE 10 and 11). Members of the DHVE group commonly occurred across the chimney transect and were detected as major components in several exterior samples (Fig. 4a, Table S1). Until now, this group was composed entirely of uncultured environmental sequences, and little is known about their physiological characteristics because of the lack of pure cultures. Phylotype Q3-A38 showed 94% sequence similarity to *Aciduliprofundum boonei*, an obligate thermoacidophilic S- or Fe-reducing heterotroph capable of growth at pH 3.3 to 5.8 and between 55 and 75°C (Reysenbach et al. 2006).

In addition, several phylotypes detected in samples P3, Q1, and Q2 fell into the order *Thermoproteales* (Fig. 4, Table S1). They aligned closely with clones or cultures recovered from hydrothermal chimneys (Pagé et al. 2004), geothermal wells on Vulcano Island (Rogers & Amend 2005), and high-temperature basaltic flanks in the East Pacific Rise (Ehrhardt et al. 2007). With increasing investigations, it was suggested that the *Thermoproteales* might commonly exist and play a potentially significant role in different hydrothermal habitats (Kormas et al. 2006, Ehrhardt et al. 2007, Nunoura et al. 2010). Only 1 phylotype affiliated with the order *Archaeoglobales* was detected from sample P2.

Bacterial phylotypes

Bacterial phylotypes were classified into the following phyla and uncultured groups: *Proteobacteria* (including *Alpha-*, *Beta-*, *Gamma-*, *Delta-*, and *Epsilonproteobacteria*), *Planctomycetes*, *Chloroflexi*, *Bacteroidetes*, *Spirochaetes*, *Deinococcus-Thermus*, *Cyanobacteria*, *Firmicutes*, OP1, and OP11 (Teske et al. 2002). Their phylogenetic positions are shown in Figs. 6 & 7, and in Fig. S2 and Table S2 in the Supplement. Members of the phylum *Proteobacteria* were the most dominant group in the *Bacteria* domain (Fig. 4b, Table S2).

Epsilonproteobacteria

Members within the *Epsilonproteobacteria* group were frequently detected in all 9 samples. Phylo-

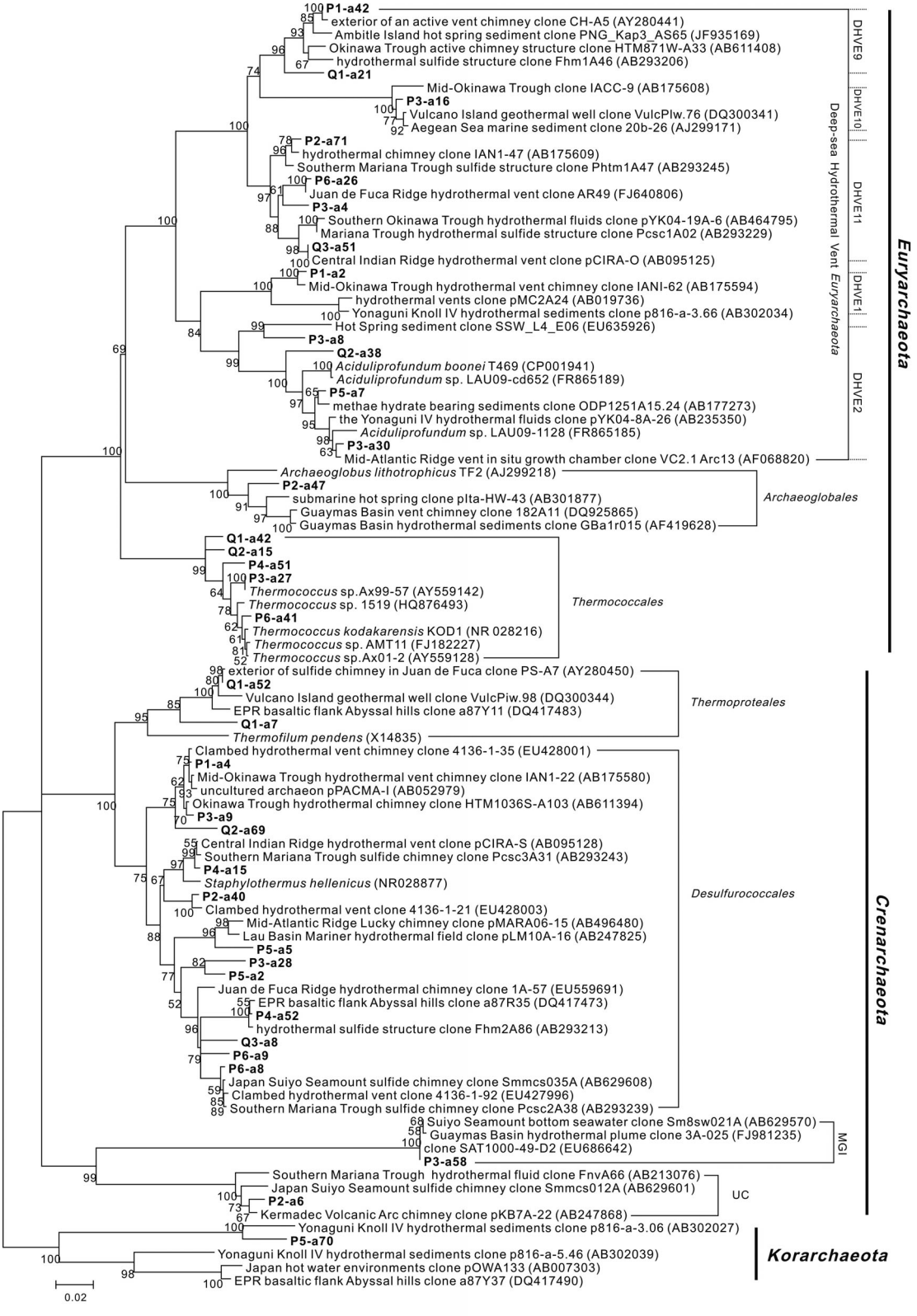

Fig. 5. Phylogenetic relationships of representative archaeal clones obtained from the Dudley black smoker chimney. The tree was inferred by neighbor-joining analysis of 16S rRNA gene sequences with Mega (5.0). Clones from this study are denoted in **bold**. Numbers in parentheses are the GenBank accession numbers for sequences obtained from NCBI, excluding our clones. Bootstrap percentages were obtained by using 1000 replicates, and values >50% are indicated at the nodes. The scale bar represents the expected number of changes per nucleotide position. MGI: marine group I; UC: unclassified

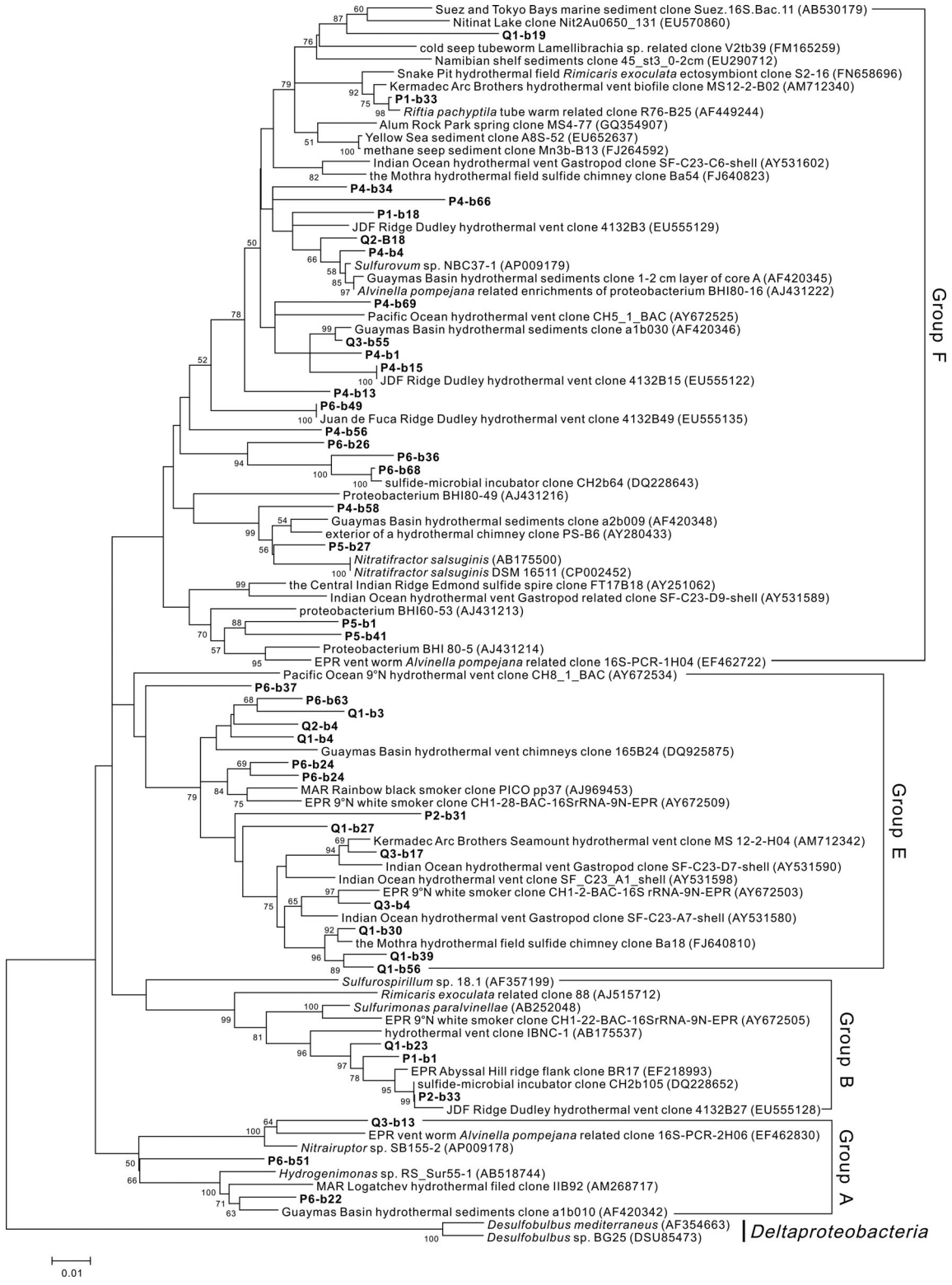

Fig. 6. Phylogenetic tree based on the 16S rRNA gene of *Epsilonproteobacteria*. The tree was inferred by neighbor-joining analysis of 16S rRNA gene sequences with Mega (5.0). Clones from this study are denoted in **bold**. Numbers in parentheses are the GenBank accession numbers for sequences obtained from NCBI, excluding our clones. Bootstrap percentages were obtained by using 1000 replicates, and values >50% are indicated at the nodes. The scale bar represents the expected number of changes per nucleotide position

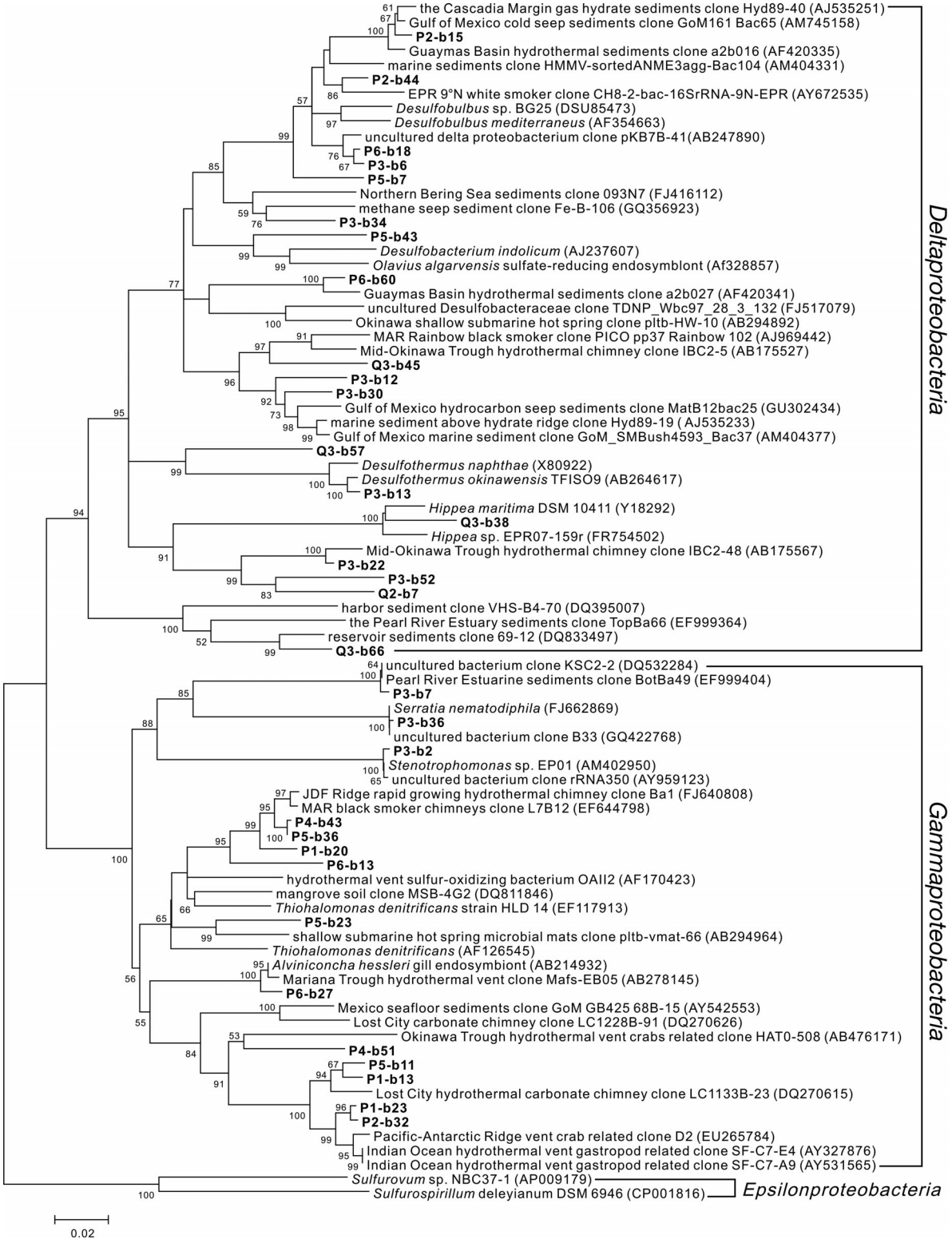

Fig. 7. Phylogenetic tree based on the 16S rRNA genes of *Gamma*- and *Deltaproteobacteria*. The tree was inferred by neighbor-joining analysis of 16S rRNA gene sequences with Mega (5.0). Clones from this study are denoted in **bold**. Numbers in parentheses are the GenBank accession numbers for sequences obtained from NCBI, excluding our clones. Bootstrap percentages were obtained by using 1000 replicates, and values >50% are indicated at the nodes. The scale bar represents the expected number of changes per nucleotide position

genetically, these phylotypes were classified into 4 different subgroups (A, B, E, and F) based on the 7-group division proposal of Corre et al. (2001).

Three phylotypes, P6-b22, P6-b51, and Q3-b13, fell into group A (Fig. 6) which were only detected in samples P6 (6 clones) and Q3 (1 clone). The genus *Nitratiruptor* contains the cultured representatives of this group (Nakagawa et al. 2005a,b). Generally, these organisms are strict thermophilic chemolithoautotrophs growing optimally at 55°C (Nakagawa et al. 2005b). Phylotypes in group B were commonly found across the chimney transect, except samples P3 and P6 (Table S2). In particular, members of group B dominated the middle layers P2 and Q2 with more than 50% in their bacterial libraries (Fig. 4b). Our phylotypes exhibited highest similarities to environmental sequences obtained mainly from hydrothermal chimneys (Nagakawa et al. 2005c, Zhou et al. 2009) and near a crustal flank (Ehrhardt et al. 2007). To date, only the genus *Sulfurimonas* (Fig. 6) was included in group B. In general, members of genus *Sulfurimonas* grow chemolithoautotrophically with sulfide, S^0, thiosulfate, and H_2 as electron donors (Takai et al. 2006).

Among group E, we found that most representative phylotypes formed a cluster with sequences from hydrothermal niches, including chimneys of the Juan de Fuca Ridge (Wang et al. 2009, Zhou et al. 2009), a white smoker in East Pacific Rise 9° N (Kormas et al. 2006), vents in Brothers Seamount, and some epibionts of vent invertebrates (Alain et al. 2002, Goffredi et al. 2004). Members of group E were the most abundant components in samples P6, Q1, and Q3 (Fig. 4b, Table S2). Members of the genus *Sulfurospirillum* were also classified into group E (Corre et al. 2001, Alain et al. 2002), which utilize sulfur or thiosulfate as electron donors (Straub & Schink 2004).

In total, 21 phylotypes fell into group F (Fig. 6). No sequence of this group was detected in sample P3, and there were only 1 or 2 clones in samples P2 and Q1. In contrast, samples P4 and P5 contained the most abundant clones of this group, which accounted for up to 45% of the bacterial libraries (Table S2). A number of clones in group F had relatives closest to epibionts of vent invertebrates (tube worms, gastropods, and shrimp; Goffredi et al. 2004, Grzymski et al. 2008) as well as environmental sequences retrieved from vents and surrounding niches (Fig. 6). Isolates in the genera *Sulfurovum* and *Nitratifractor* were recently reported as cultured species in group F (Inagaki et al. 2004, Nakagawa et al. 2005c).

Delta- and *Gammaproteobacteria*

No *Deltaproteobacteria* were detected in the bacterial libraries of the outer wall samples, P1 and Q1. In total, 18 phylotypes (representing 44 clones) constituted the *Deltaproteobacteria* cluster. Their distributions varied greatly: most *Deltaproteobacteria* clones were found in the inner layer samplers P3 and Q3, in which they accounted for about 25 and 18% of the detected bacterial clones, in contrast to 4~7% in other samples (Fig. 4, Table S2). These phylotypes were closely (94% or higher similarity) related to cultured members of the family *Desulfobulbaceae* (Sass et al. 2002, Teske et al. 2002), members of the genus *Desulfothermus* (Nunoura et al. 2007), and uncultured sequences of several distinct branches within *Deltaproteobacteria* (Fig. 7). Generally, members of the *Deltaproteobacteria* are mainly anaerobic chemoorganotrophic sulfate-reducers capable of utilizing sulfate, nitrate, and ferric iron as electron acceptors (Kato et al. 2009). However, members of the genus *Hippea*, which were mainly isolated from seafloor hydrothermal vents, were described as being unable to grow by sulfate reduction but rather by sulfur reduction (Flores et al. 2012).

The exterior samples P1 and Q1 contained 14 phylotypes within the *Gammaproteobacteria*, and were the main habitats of this group. Most phylotypes branched among uncultivated clones from a carbonate chimney (Brazelton et al. 2006), a high temperature black smoker (Wang et al. 2009), and marine and estuarine sediments (Martinez et al. 2006, Jiang et al. 2009). Several phylotypes were closely related to sequences recovered from sulfur-oxidizing bacterial endosymbionts of bivalves or gastropods at hydrothermal vents and cold seeps (Fig. 7).

Other bacterial phylotypes

Two phylotypes, Q1-b63 and P6-b16, were members of thermophilic bacteria in the order *Thermales* (Fig. S2). In particular, P6-b16 was closely related (>98% sequence similarity) to *Oceanithermus profundus*, a thermophilic (optimal growth at 60°C), microaerophilic, facultatively chemolithotrophic bacterium isolated from the 13° N East Pacific Rise hydrothermal vents (Miroshnichenko et al. 2003, Kormas et al. 2006). Three phylotypes, which were detected exclusively in the inner sample P3, belonged to the *Firmicutes*. Phylotypes within other bacterial lineages were retrieved in low numbers, including members of *Chloroflexi* (1 OTU for 1 clone),

Spirochaetes (2 OTUs for 2 clones), *Cyanobacteria* (2 OTUs for 2 clones), *Planctomycetes* (3 OTUs for 10 clones), *Alphaproteobacteria* (5 OTUs for 5 clones), and the uncultured OP1, OP11 candidate divisions (1 OTU for 1 clone, respectively).

Statistical analysis

Archaeal and bacterial 16S rDNA clone libraries of different chimney parts were subjected to PCA together. Results of the PCA showed that 9 samples were grouped into several different clusters comparable with their phylogenetic datasets (Fig. 8). According to the PCA plot, samples P1 and Q1 formed 1 group, P3 formed a distinct group, and the rest of the samples (P2, P4, Q2, P5, P6, and Q3) formed a third group. The first 2 principal components (PC1 and PC2) explained 65.21 % of the total variation.

DISCUSSION

Spatial variations of microbial communities in different chimney zones

Diverse microbial communities were detected from our active hydrothermal sulfide chimney. Microbial compositions and biomass shifted dramatically from the exterior to the interior of the chimney and formed obvious microbial zones at different spatial positions. Quantitative analysis showed that density of bacterial cells detected from the outer (~10^7 cells g^{-1}) to inner parts (only ~10^4 cells g^{-1}) varied by at least 3 orders of magnitude, while archaeal biomass did not fluctuate over a wide range (about 10^5–10^6 cells g^{-1}; Fig. 3 and Table S3 in the Supplement). It is conceivable that exposure to cold seawater makes the exterior wall of the chimney a relatively low-temperature environment where mesophilic bacteria flourish. In contrast, the inner parts are likely too hot to provide a niche for bacteria, whereas archaea could adapt to such environments with their higher thermoadaptability (Kelley et al. 2002). Correspondingly, we observed a dramatic shift in the compositions of microbial communities within different microenvironments, from predominantly mesophilic, sulfur-oxidizing bacterial communities at the outer surfaces to thermophilic or hyperthermophilic, archaeal sulfur-reducers in the inner layers of the chimney, as follows.

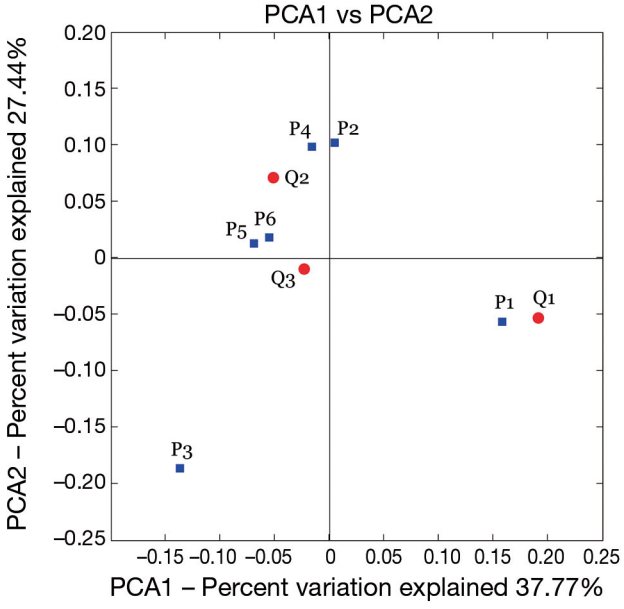

Fig. 8. Principal component analysis of different microbial 16S rRNA gene clone libraries. Squares indicate samples obtained from the P conduit and circles indicate samples obtained from the inactive Q conduit of the Dudley black smoker chimney (see Fig. 2 for conduit and subsampling locations)

In the exterior surfaces (P1 and Q1), microbial composition and community structure were characterized by the predominance of the *Epsilon-* and *Gammaproteobacteria* and the archaeal members of the DHVE group. Results of PCA showed that they hosted very similar microbial populations and community structures (Fig. 8) and also harbored roughly equal biomass (Fig. 3, Table S3). The bacterial groups were mainly composed of autotrophic mesophilic species (Inagaki et al. 2003), whose metabolism is closely related to sulfur cycles with a wide spectrum of substrates such as $S_2O_3^{2-}$ and S^0 and with H_2S as the ultimate metabolite. In particular, some members of the *Gammaproteobacteria* could directly oxidize H_2S using oxygen, which is the most direct approach for obtaining energy to support chemosynthesis-based faunal communities such as tube worms, shrimps, and gastropods (Fig. 7). In contrast, the high proportion of the DHVE groups in these parts is unexpected. Generally, habitats for the DHVE group are restricted to high-temperature niches (Hoek et al. 2003, Reysenbach et al. 2006, Nunoura et al. 2010). Recently, the first cultured representative of the DHVE 2 group, *Aciduliprofundum boonei*, has also been shown to respond favorably to high temperature (55~75°C, growing best at 70°C). It is plausible that outward advection of hydrothermal fluids could still maintain some niches with high temperature which may be suitable for the survival of hyperthermophilics (Kormas et al. 2006). Members of

the *Thermococcales* and *Desulfurococcales* occurred in the exterior parts (P1 and Q1), albeit in low proportions, which again supports this hypothesis. Another possibility is that some individuals within the DHVE groups may have a non-hyperthermophilic lifestyle and can exist in those habitats that probably are not too hot (Nercessian et al. 2003, Nunoura et al. 2010).

Compared to the exterior walls, microbial communities inhabiting the middle layers shifted more dramatically (Fig. 4). According to the PCA, samples from the middle layers clustered together and formed a distinct group (Fig. 8). The archaeal components shifted from predominantly DHVE groups to *Thermococcales* (up to about 70% in the clone library). Meanwhile, other archaeal groups such as the *Desulfurococcales* also increased compared to the exterior samples. All microorganisms of the orders *Thermococcales* and *Desulfurococcales* are putative hyperthermophilics which generally show maximal growth at temperatures above 90°C (Zillig & Reysenbach 2001, Kashefi & Lovely 2003). The prevalence and predominance of these hyperthermophilic groups indicated that they were probably affected by high-temperature hydrothermal fluids. However, the occurrence of some given microbial groups indicates that there are likely more dynamic and complex environments in the middle layers of the chimney. The detection of members of the *Archaeoglobales* and *Deltaproteobacteria*, which depend on dissimilatory sulfate reduction (Jørgensen et al. 1992), suggests the presence of a seawater-derived electron acceptor, SO_4^{2-}, in the middle layers. In the domain *Bacteria*, *Epsilonproteobacteria* was the dominant eubacterial group (nearly 80% in our bacterial clone library), and pure cultures with high sequence similarity to our OTUs are generally mesophiles that grow optimally at moderate temperatures ranging between 20 and 45°C (Campbell et al. 2006). Considering all of these phenomena, plus the high porosity (P4 and P5, shown in Fig. 2), we concluded that there was intense mixing between hot hydrothermal fluids and cold seawater in the middle layers (Schrenk et al. 2003) which may have created diverse niches with different physicochemical conditions, thereby supporting the abundant and diverse microbial communities.

The inner layers P3 and Q3, where temperature was high because of their proximity to the central fluid conduits, were predominantly inhabited by archaeal populations. Archaeal biomass was about 2.22 and 2.49×10^5 cells g^{-1} (Table S3) and hyperthermophilic groups such as the *Thermococcales* and *Desulfurococcales* were predominant among archaeal communities (Fig. 4a). Furthermore, the proportion of the *Desulfurococcales* increased dramatically while relatively low-temperature DHVE decreased from the exterior walls (P1, Q1) to the inner parts (Fig. 4), which corresponds well to the varying profile of temperature across the chimney walls. In contrast, bacterial density decreased more sharply than archaeal density, to only about 10^4 cells g^{-1}. However, bacterial components in P3 and Q3 consisted of relatively diverse microbial populations, related mostly to mesophilic isolates (Fig. 4b). The occurrence of these non-thermophilic eubacterial populations, which represented minor proportions of the libraries, suggests the transport of microbial components from outer parts to inner layers through pores and cracks, likely caused by the penetration of seawater. Another possibility is that some of the bacterial populations come from seawater contamination during sampling. After sampling, hot pore fluids within the chimney cooled and contracted, which caused the entrainment of ambient seawater into the spire (Kormas et al. 2006). The detection of *Cyanobacteria* which obtain their energy through photosynthesis from the inner layer P3 indicated the influence of the surface seawater during the recovery of the sulfide chimney from the seafloor to the ship. Although we classified P3 and Q3 into the same group according to their spatial position, they were differentiated by PCA (Fig. 8), suggesting the presence of different microbial community structures even in similar spatial locations of the chimney. It is not difficult to understand this when taking into consideration the difference between the P and Q conduits. As noted before, the P conduit was still active and venting high-temperature fluids, whereas the Q conduit was essentially inactive and filled with minerals, indicating relatively lower temperature than the P conduit. Therefore, spatial location (inner vs. outer layer) and activity (active vs. inactive) of structural components of a chimney dictate the microbial community composition and structure.

Factors potentially affecting microbial distribution within the chimney

Within the hydrothermal chimney walls, environmental conditions at different spatial locations such as *in situ* temperature, fluid geochemistry, mineralogical framework, and porosity are potential constraints on microbial populations and their distributions (Edwards et al. 2003, Kormas et al. 2006). *In situ* temperature is probably one of the most important

parameters that exerts a key, first-order control on microbial populations, diversity, and community structure (Pagé et al. 2008, Schrenk et al. 2008). The temperature regime from the center to the edge of a chimney is commonly approximated by a decreasing profile based on the conductive cooling model (Tivey & McDuff 1990). Thus, it is not hard to understand that there was a visible shift within the walls in resident microbes, from mesophilic eubacterial communities to hyperthermophilic archaea along the transect with approaching proximity to the central high-temperature conduits (Figs. 3 & 4). Moreover, similar population shifts also occurred for archaeal dwellers. From the exterior to the interior of the Dudley chimney, the dominant communities transitioned gradually from the DHVE (P1 and Q1) to *Thermococcales* (middle layers) and to *Desulforococcales* (P3, Q3). Interestingly, the shift in growth temperatures of archaeal pure cultures which were closely related to our phylotypes, from 50~75°C (optimal 70°C) for *Aciduliprofundum boonei* in the DHVE group (Reysenbach et al. 2006), 55~95°C (optimal 80~90°C) for the those of the genus *Thermococcus* within the *Thermococcales* (Zillig & Reysenbach 2001), to 80~121°C (optimal 85~106°C) for different genera within the *Desulfurococcales* (Huber & Stetter 2001), correlates well with the increasing temperature across the chimney wall. Even in the middle layers, the inner parts (P4, P5) with relatively higher temperature accommodated higher proportions of *Desulfurococcales* than the outer parts (P2, Q2). The trend of increasing growth temperatures of dominant archaea from the exterior to the interior indicated that microbes in the chimney walls were likely affected by temperature.

Geochemical characteristics of vent fluids through the chimney walls also play an important role in the selection for microbial communities by varying carbon source and electron donors and acceptors. According to our results, it can be inferred that microbes with metabolism involving sulfur compounds (including SO_4^{2-}, $S_2O_3^{2-}$, S^0, and H_2S) are common and pivotal to sustain the chimney microbial communities. Furthermore, microbes with different metabolic processes of sulfur (sulfur/sulfide-oxidation and sulfate reduction) occurred from the surface to near the center portions of the chimney at varying distances of merely centimeters. This can be attributed in large part to the sharp transition from oxidized conditions dominated by seawater at the surface to reduced conditions dictated by hydrothermal fluids across the chimney walls (McCollom & Shock 1997). As mentioned above, chimney exteriors are exposed to cold, neutral, and oxic seawater, and correspondingly, members of mesophilic and aerobic sulfide- or sulfur-oxidizers such as *Gamma-* and *Epsilonproteobacteria* dominate in these positions (P1 and Q1). These microorganisms have the ability to oxidize reduced sulfur species using O_2 or NO_3^- as electron acceptors (López-García et al. 2003). Conversely, the inner layers (P3 and Q3) with close proximity to the hydrothermal fluid are hot, anoxic habitats where sulfur-reduction is energetically favored. Resident microbial communities consisted exclusively of anaerobic, strictly reduced sulfur-dependent archaea (*Desulfurococcales* and *Thermococcales*; Fig. 4a). Although the middle layers are not directly in contact with hydrothermal fluids or seawater, pores and fissures in the chimney walls (shown in Fig. 2) allow the encounter and extensive mixing of reduced vent fluids and oxidizing seawater. The mixing process forms a dynamic and complex environment (such as P4) where both hydrothermal fluids and seawater exert an important influence on microbial populations. Therefore, it is not surprising to find that microbial populations that predominantly occur in the exterior and inner part coexist in the middle layers. Therefore, we can infer that microbial populations and their distributions are linked to fluid features, varying from mesophilic, sulfur-oxidizing bacterial communities (*Gamma-* and *Epsilonproteobacteria*) at the outer layers to thermophilic, archaeal sulfur-reducers (*Thermococcales*, *Archaeoglobales*, *Desulfurococcales*, and *Thermoproteales*) in the interior part of the chimney.

Organic substrates probably contributed greatly to sustain microbial communities inhabiting the chimney, since heterotrophic populations accounted for a large proportion of the microbial communities (Fig. 4). Within the *Deltaproteobacteria*, clones fell into different lineages such as the *Desulfobulbaceae*, *Desulfobacteraceae*, *Desulfohalobiaceae*, and *Desulfurellaceae*. Although their growth temperatures and electron acceptor preferences differ, these microbes are generally chemoorganotrophic and utilize organic substrates to grow. Among our archaeal clones, those related to the cultured *Thermococcales* and *Desulfurococcales* are also heterotrophs and require organic compounds for growth. Although organic carbon could come from different sources, and it is difficult to quantitatively estimate the contributions of organic compounds (Kormas et al. 2006), the organic compounds originating from *in situ* microbes within the chimney matrix probably played an important role in feeding heterotrophic populations.

Environmental regimes within the chimney walls

Environmental regimes within the chimney walls were further distinguished by integrating mineralogy, fluid geochemistry, microbial communities, and their distribution profiles (see Fig. 2 for details). As shown by previous reports, hydrothermal chimneys are characterized by steep physical and chemical gradients at small spatial scales, and corresponding to these gradients, microbial communities also vary dramatically (Takai & Horikoshi 1999, Schrenk et al. 2003, Kormas et al. 2006). Thus far, it is still difficult to measure *in situ* environmental parameters within the chimney walls, although several different models have been proposed (Tivey & McDuff 1990, Kormas et al. 2006). Alternatively, microbial communities and their distribution patterns may yield insights into environmental parameters of their habitats, and consequently, basic environmental schematics could be inferred based on microbial physiological and metabolic traits. In several similar investigations, temperature regimes within the chimney walls were estimated on the basis of the temperatures at which different mineral assemblages form (Schrenk et al. 2003, Kormas et al. 2006). However, it should be pointed out that the temperature at which minerals form cannot reflect the actual *in situ* temperature experienced by those resident microorganisms. For instance, the lowest temperature for the formation of most sulfide minerals is generally higher than 150°C, and it is impossible for microbes to survive at such high temperatures. We therefore used the growth temperatures of thermophilic or hyperthermophilic archaeal groups rather than the formation temperature of different mineral assemblages as temperature indicators to outline the likely *in situ* temperature ranges for different chimney layers (Fig. 2). Pagé et al. (2008) deployed thermocouple arrays on the active vents at Guaymas Basin to record *in situ* temperatures at which microorganisms colonize the associated mineral deposits and detected inhabited microbes. There was a good coherence between *in situ* measured temperature and growth temperature of detected archaea, which suggests that microbial physiological characteristics can be used to infer *in situ* temperature schematics in the chimney walls. Thus, on the basis of physiological features of cultured relatives of our clones, together with the surface temperature inferred by Kormas et al. (2006), the *in situ* temperature can be estimated to be 15~40°C at the outer surfaces (Fig. 2a), 40~90°C in the middle layers (Fig. 2b,c), and ≤120°C in the interior layers (Fig. 2d). As such, a steep temperature variation from 120 to 330°C existed on a very small scale (central conduits P0, ca. 5 cm; Fig. 2e).

Some clues about the mixing of hydrothermal fluids and seawater within the chimney walls could be gained from microbial physiological and metabolic traits, especially those indicative of terminal electron-accepting processes. For instance, although bacterial biomass was lowest in samples P3 and Q3, which were adjacent to the central channels, the proportions of *Deltaproteobacteria* were the highest in the bacterial libraries (Fig. 4b). In fact, members of *Deltaproteobacteria* are well known to be typical sulfate reducers which utilize SO_4^{2-} as the necessary electron acceptor to obtain metabolic energy (Jørgensen et al. 1992), although the only source of sulfate in vent chimneys is from seawater. The detection of *Deltaproteobacteria* in the inner parts of the chimney therefore signifies the percolation of seawater. Hence, it can be inferred that, even near the central parts of the chimney where hydrothermal fluids dominate the environments, seawater can penetrate into the far interior portions through cracks, fractures, and interspaces (Fig. 2d). Similarly, some hyperthermophilic microbes could be used as excellent temperature indicators because they will not survive when the temperature is below their minimum growth temperatures (Holden et al. 1998, Kelley et al. 2002). The occurrence of phylotypes affiliated to the *Thermococcales* and *Desulfurococcales* indicates that hydrothermal fluids can reach the area near the exterior surface through outward convection since it is impossible to sustain relatively high temperatures (above 60°C) solely by means of conductive cooling (Fig. 2a) (Tivey & McDuff 1990, Kormas et al. 2006). In the middle cylinder, especially the inner zones (P4, P5, P6) where interspaces and fractures are abundant, inward penetration of seawater and outward percolation of hot hydrothermal fluid would cause intensive mixing as shown in Fig. 2b,c.

CONCLUSIONS

In this study, we determined the mineralogy, microbial community structure, and their distribution patterns in different spatial microhabitats of a chimney wall recovered from the Dudley site of the Main Endeavour Field in the Juan de Fuca Ridge. Our results showed that the chimney wall exhibited a clear zonation in mineralogy, fluid geochemistry, and microbiology. From the exterior to the interior of the chimney structure, mineral composition varied from predominantly marcasite and pyrite to a high abun-

dance of chalcopyrite and pyrite with smaller amounts of wurtzite and sphalerite. Likewise, the chimney exhibited layered microbial composition and community structure, from predominantly aerobic, sulfur-oxidizing mesophilic *Gamma-* and *Deltaproteobacteria* in the outer layer to mostly anaerobic, sulfur-reducing thermophilic and hyperthermophilic *Thermococcales* and *Desulfurococcales* in the inner layers. Yet, microbial communities differed between mineral-filled and actively venting conduits within the chimney. Given these results, an attempt was made to estimate the *in situ* temperature across the chimney walls on the basis of the growth temperatures of those dominant microbial groups. However, hydrothermal chimneys are extremely heterogeneous, complicated, and dynamic, so it is often very difficult to exactly elucidate the real conditions inside the walls. Further research should be carried out and new methods should be developed to obtain more *in situ* data on environmental parameters and correlate this data with that of *in situ* microbes.

Acknowledgements. This work was financially supported by the National Basic Research Program of China (973 Program, No. 2012CB417300), the National Natural Science Foundation of China (NSFC, Nos. 41002122 and 41373071), and the Fundamental Research Funds for the Central Universities. We greatly appreciate the efforts and assistance of Maurice Tivey, Marv Lilly, Kang Ding, and all crew members of RV 'Atlantis' / DSV 'Alvin', which made the Joint Sino-US cooperative cruise AT11-31 a success.

LITERATURE CITED

Alain K, Olagnon M, Desbruyeres D, Pagé A and others (2002) Phylogenetic characterization of the bacterial assemblage associated with mucous secretions of the hydrothermal vent polychaete *Paralvinella palmiformis*. FEMS Microbiol Ecol 42:463–476

Bano N, Ruffin S, Ransom B, Hollibaugh JT (2004) Phylogenetic composition of Arctic Ocean archaeal assemblages and comparison with Antarctic assemblages. Appl Environ Microbiol 70:781–789

Blöchl E, Rachel R, Burggraf S, Hafenbradl D, Jannasch HW, Stetter KO (1997) *Pyrolobus fumarii*, gen. and sp. nov., represents a novel group of archaea, extending the upper temperature limit for life to 113°C. Extremophiles 1:14–21

Brazelton WJ, Schrenk MO, Kelley DS, Baross JA (2006) Methane- and sulfur-metabolizing microbial communities dominate the Lost City hydrothermal field ecosystem. Appl Environ Microbiol 72:6257–6270

Butterfield DA, McDuff RE, Mottl MJ, Lilley MD, Lupton JE, Massoth GJ (1994) Gradients in the composition of hydrothermal fluids from the Endeavour Segment vent field: phase separation and brine loss. J Geophys Res 99: 9561–9583

Campbell BJ, Engel AS, Porter ML, Takai K (2006) The versatile ε-proteobacteria: key players in sulphidic habitats. Nat Rev Microbiol 4:458–468

Corre E, Reysenbach AL, Prieur D (2001) Epsilon-proteobacterial diversity from a deep-sea hydrothermal vent on the Mid-Atlantic Ridge. FEMS Microbiol Lett 205:329–335

Delaney JR, Robigou V, McDuff RE, Tivey MK (1992) Geology of a vigorous hydrothermal system on the Endeavour Segment, Juan de Fuca Ridge. J Geophys Res 97: 19663–19682

DeSantis TZ Jr, Hugenholtz P, Keller K, Brodie EL and others (2006) NAST: a multiple sequence alignment server for comparative analysis of 16S rRNA genes. Nucleic Acids Res 34:W394–W399

Dilly O, Bloem J, Vos A, Munch JC (2004) Bacterial diversity in agricultural soils during litter decomposition. Appl Environ Microbiol 70:468–474

Edwards KJ, McCollom TM, Konishi H, Buseck PR (2003) Seafloor bioalteration of sulfide minerals: results from in situ incubation studies. Geochim Cosmochim Acta 67: 2843–2856

Ehrhardt CJ, Haymon RM, Lamontagne MG, Holden PA (2007) Evidence for hydrothermal Archaea within the basaltic flanks of the East Pacific Rise. Environ Microbiol 9:900–912

Emerson D, Moyer CL (2002) Neutrophilic Fe-oxidizing bacteria are abundant at the Loihi Seamount hydrothermal vents and play a major role in Fe oxide deposition. Appl Environ Microbiol 68:3085–3093

Flores GE, Hunter RC, Liu YT, Mets A, Schouten S, Reysenbach AL (2012) *Hippea jasoniae* sp. nov. and *Hippea alviniae* sp. nov., thermoacidophilic members of the class *Deltaproteobacteria* isolated from deep-sea hydrothermal vent deposits. Int J Syst Evol Microbiol 62:1252–1258

Goffredi SK, Waren A, Orphan VJ, Van Dover CL, Vrijenhoek RC (2004) Novel forms of structural integration between microbes and a hydrothermal vent gastropod from the Indian Ocean. Appl Environ Microbiol 70: 3082–3090

Grzymski JJ, Murray AE, Campbell BJ, Kaplarevic M and others (2008) Metagenome analysis of an extreme microbial symbiosis reveals eurythermal adaptation and metabolic flexibility. Proc Natl Acad Sci USA 105: 17516–17521

Harmsen H, Prieur D, Jeanthon C (1997) Distribution of microorganisms in deep-sea hydrothermal vent chimneys investigated by whole-cell hybridization and enrichment culture of thermophilic subpopulations. Appl Environ Microbiol 63:2876–2883

Hoek J, Banta A, Hubler F, Reysenbach AL (2003) Microbial diversity of a sulphide spire located in the Edmond deep-sea hydrothermal vent field on the Central Indian Ridge. Geobiology 1:119–127

Holden JF, Summit M, Baross JA (1998) Thermophilic and hyperthermophilic microorganisms in 3–30°C fluids following a deep-sea volcanic eruption. FEMS Microbiol Ecol 25:33–41

Huber H, Stetter KO (2001) Desulfurococcales. ord. nov. In: Boone DR, Castenholz RW (eds) Bergey's manual of systematic bacteriology, 2nd edn, Vol 1. The *Archaea* and the deeply branching and phototrophic *Bacteria*. Springer, New York, NY, p 170–179

Huber T, Faulkner G, Hugenholtz P (2004) Bellerophon: a program to detect chimeric sequences in multiple sequence alignments. Bioinformatics 20:2317–2319

Huber JA, Butterfiled DA, Baross JA (2006) Diversity and distribution of subseafloor Thermococcales populations

in diffuse hydrothermal vents at an active deep-sea volcano in the northeast Pacific Ocean. J Geophys Res 111, G04016, doi:10.1029/2005JG000097

Inagaki F, Takai K, Kobayashi H, Nealson KH, Horikoshi K (2003) *Sulfurimonas autotrophica* gen. nov., sp. nov., a novel sulfur-oxidizing ε-proteobacterium isolated from hydrothermal sediments in the Mid-Okinawa Trough. Int J Syst Evol Microbiol 53:1801–1805

Inagaki F, Takai K, Nealson KH, Horikoshi K (2004) *Sulfurovum lithotrophicum* gen. nov., sp. nov., a novel sulfur-oxidizing chemolithoautotroph within the ε-*Proteobacteria* isolated from the Okinawa Trough hydrothermal sediments. Int J Syst Evol Microbiol 54:1477–1482

Jiang LJ, Zheng YP, Peng XT, Zhou HY, Zhang CL, Xiao X, Wang FP (2009) Vertical distribution and diversity of sulfate-reducing prokaryotes in the Pearl River estuarine sediments, Southern China. FEMS Microbiol Ecol 70: 249–262

Jørgensen BB, Isaksen MF, Jannasch HW (1992) Bacterial sulfate reduction above 100°C in deep-sea hydrothermal vent systems. Science 258:1756–1757

Kashefi K, Lovely DR (2003) Extending the upper temperature limit for life. Science 301:934

Kato S, Kobayashi C, Kakegawa T, Yamagishi A (2009) Microbial communities in iron-silica-rich microbial mats at deep-sea hydrothermal fields of the Southern Marina Trough. Environ Microbiol 11:2094–2111

Kelley DS, Baross JA, Delaney JR (2002) Volcanoes, fluids, and life at mid-ocean ridge spreading centers. Annu Rev Earth Planet Sci 30:385–491

Kormas KA, Tivey MK, Von Damm K, Teske A (2006) Bacterial and archaeal phylotypes associated with distinct mineralogical layers of a white smoker spire from a deep-sea hydrothermal vent site (9° N, East Pacific Rise). Environ Microbiol 8:909–920

Larkin MA, Blackshields G, Brown NP, Chenna R and others (2007) Clustal W and Clustal X version 2.0. Bioinformatics 23:2947–2948

Lee ZMP, Bussema C, Schmidt TM (2009) rrnDB: documenting the number of rRNA and tRNA genes in bacteria and archaea. Nucleic Acids Res 37:D489–D493

Li J, Zhou H, Peng X, Wu Z, Chen S, Fang J (2012) Microbial diversity and biomineralization in low-temperature hydrothermal iron-silica-rich precipitates of the Lau Basin hydrothermal field. FEMS Microbiol Ecol 81: 205–216

Lloyd KG, May MK, Kevorkian RT, Steen AD (2013) Meta-analysis of quantification methods shows that archaea and bacteria have similar abundances in the subseafloor. Appl Environ Microbiol 79:7790–7799

López-García P, Duperron S, Philippot P, Foriel J, Susini J, Moreira D (2003) Bacterial diversity in hydrothermal sediment and epsilonproteobacterial dominance in experimental microcolonizers at the Mid-Atlantic Ridge. Environ Microbiol 5:961–976

Lozupone C, Knight R (2005) Unifrac: an online tool for comparing microbial communities. Appl Environ Microbiol 71:8228–8235

Martin-Cuadrado AB, Rodriguez-Valera F, Moreira D, Alba JC and others (2008) Hindsight in the relative abundance, metabolic potential and genome dynamics of uncultivated marine archaea from comparative metagenomic analyses of bathypelagic plankton of different oceanic regions. ISME J 2:865–886

Martinez RJ, Mills HJ, Story S, Sobecky PA (2006) Prokaryotic diversity and metabolically active microbial populations in sediments from an active mud volcano in the Gulf of Mexico. Environ Microbiol 8:1783–1796

McCliment EA, Voglesonger KM, O'Day PA, Dunn EE, Holloway JR, Cary SC (2006) Colonization of nascent, deep-sea hydrothermal vents by a novel Archaeal and Nanoarchaeal assemblage. Environ Microbiol 8:114–125

McCollom TM (2000) Geochemical constraints on primary productivity in submarine hydrothermal vent plumes. Deep-Sea Res I 47:85–101

McCollom TM, Shock EL (1997) Geochemical constrainst on chemolithoautotrophic metabolism by microorganisms in seafloor hydrothermal systems. Geochim Cosmochim Acta 61:4375–4391

Miroshnichenko ML, L'Haridon S, Jeantho C, Antipov AN and others (2003) *Oceanithermus profundus* gen. nov., sp. nov., a thermophilic, microaerophilic, facultatively chemolithoheterotrophic bacterium from a deep-sea hydrothermal vent. Int J Syst Evol Microbiol 53:747–752

Nakagawa S, Takai K, Inagaki F, Hirayama H, Nunoura T, Horikoshi K, Sako Y (2005a) Distribution, phylogenetic diversity and physiological characteristics of epsilon-*Proteobacteria* in a deep-sea hydrothermal field. Environ Microbiol 7:1619–1632

Nakagawa S, Takai K, Inagaki F, Horikoshi K, Sako Y (2005b) *Nitratiruptor tergarcus* gen. nov., sp. nov. and *Nitratifractor salsuginis* gen. nov., sp. nov., nitrate-reducing chemolithoautotrophs of the epsilon-*Proteobacteria* isolated from a deep-sea hydrothermal system in the Mid-Okinawa Trough. Int J Syst Evol Microbiol 55:925–933

Nakagawa S, Takai K, Inagaki F, Chiba H and others (2005c) Variability in microbial community and venting chemistry in a sediment-hosted backarc hydrothermal system: impacts of subseafloor phase-separation. FEMS Microbiol Ecol 54:141–155

Nakagawa T, Takai K, Suzuki Y, Hirayama H, Konno U, Tsunogai U, Horikoshi K (2006) Geomicrobiological exploration and characterization of a novel deep-sea hydrothermal system at the TOTO caldera in the Mariana Volcanic Arc. Environ Microbiol 8:37–49

Nercessian O, Reysenbach AL, Prieur D, Jeanthon C (2003) Archaeal diversity associated with *in situ* samplers deployed on hydrothermal vents on the East Pacific Rise (13° N). Environ Microbiol 5:492–502

Nunoura T, Takai K (2009) Comparison of microbial communities associated with phase-separation-induced hydrothermal fluids at the Yonaguni Knoll IV hydrothermal field, the Southern Okinawa Trough. FEMS Microbiol Ecol 67:351–370

Nunoura T, Oida H, Miyazaki M, Suzuki Y, Takai K, Horikoshi K (2007) *Desulfothermus okinawensis* sp. nov., a thermophilic and heterotrophic sulfate-reducing bacterium isolated from a deep-sea hydrothermal field. Int J Syst Evol Microbiol 57:2360–2364

Nunoura T, Oida H, Nakaseama M, Kosaka A and others (2010) Archaeal diversity and distribution along thermal and geochemical gradients in hydrothermal sediments at the Yonaguni Knoll IV hydrothermal field in the Southern Okinawa Trough. Appl Environ Microbiol 76: 1198–1211

Opatkiewicz AD, Butterfield DA, Baross JA (2009) Individual hydrothermal vents at Axial Seamount harbor distinct subseafloor microbial communities. FEMS Microbiol Ecol 70:413–424

Pagé A, Juniper K, Olagnon M, Alain K, Desrosiers G,

Querellou J, Cambon-Bonavita MA (2004) Microbial diversity associated with a *Paralvinella sulfincola* tube and the adjacent substratum on an active deep-sea vent chimney. Geobiology 2:225–238

Pagé A, Tivey MK, Stakes DS, Reysenbach AL (2008) Temporal and spatial archaeal colonization of hydrothermal vent deposits. Environ Microbiol 10:874–884

Perner M, Kuever J, Seifert R, Pape T and others (2007) The influence of ultramafic rocks on microbial communities at the Logatchev hydrothermal field, located 15° N on the Mid-Atlantic Ridge. FEMS Microbiol Ecol 61:97–109

Reysenbach AL, Liu YT, Banta AB, Beveridge TJ (2006) Isolation of a ubiquitous obligate thermoacidophilic archaeon from deep-sea hydrothermal vents. Nature 442:444–447

Rogers KL, Amend JP (2005) Archaeal diversity and geochemical energy yields in a geothermal well on Vulcano Island, Italy. Geobiology 3:319–332

Sako Y, Nomura A, Uchida A, Ishida Y and others (1996) *Aeropyrum pernix* gen. nov., sp. nov., a novel aerobic hyperthermophilic archaeon growing at temperature up to 100°C. Int J Syst Bacteriol 46:1070–1077

Sass A, Rutters H, Cypionka H, Sass H (2002) *Desulfobulbus mediterraneus* sp. nov., a sulfate reducing bacterium growing on mono- and disaccharides. Arch Microbiol 177:468–474

Schloss PD, Handelsman J (2005) Introducing DOTUR, a computer program for defining operational taxonomic units and estimating species richness. Appl Environ Microbiol 71:1501–1506

Schrenk MO, Kelley DS, Delaney JR, Baross JA (2003) Incidence and diversity of microorganisms within the walls of an active deep-sea sulfide chimney. Appl Environ Microbiol 69:3580–3592

Schrenk MO, Holden JF, Baross JA (2008) Magma-to-microbe networks in the context of sulfide hosted microbial ecosystems. In: Lowell RP, Perfit MR, Seewald J, Metaxas A (eds) Magma to microbe: modeling hydrothermal processes at oceanic spreading ridges. Geophysical Monograph Vol 178. American Geophysical Union, Washington, DC, p 233–258

Straub KL, Schink B (2004) Ferrihydrite-dependent growth of *Sulfurospirillum deleyianum* through electron transfer via sulfur cycling. Appl Environ Microbiol 70: 5744–5749

Takai K, Horikoshi K (1999) Genetic diversity of archaea in deep-sea hydrothermal vent environments. Genetics 152:1285–1297

Takai K, Sako Y (1999) A molecular view of archaeal diversity in hot water environments in Japan. FEMS Microbiol Ecol 28:177–188

Takai K, Komatsu T, Inagaki F, Horikoshi K (2001) Distribution of archaea in a black smoker chimney structure. Appl Environ Microbiol 67:3618–3629

Takai K, Gamo T, Tsunogai U, Nakayama N, Hirayama H, Nealson KH, Horikoshi K (2004) Geochemical and microbiological evidence for a hydrogen-based, hyperthermophilic subsurface lithoautotrophic microbial ecosystem (HyperSLIME) beneath an active deep-sea hydrothermal field. Extremophiles 8:269–282

Takai K, Suzuki M, Nagakawa S, Miyazaki M, Suzuki Y, Inagaki F, Horikoshi K (2006) *Sulfurimonas paralvinellae* sp. nov., a novel mesophilic, hydrogen- and sulfur-oxidizing chemolithoautotroph within the *Epsilonproteobacteria* isolated from a deep-sea hydrothermal vent polychaete nest, reclassification of *Thiomicrospira denitrificans* as *Sulfurimonas denitrificans* comb. nov. and emended description of the genus *Sulfurimonas*. Int J Syst Evol Microbiol 56:1725–1733

Tamura K, Peterson D, Peterson N, Stecher G, Nei M, Kumar S (2011) MEGA5: molecular evolutionary genetics analysis using maximum likelihood, evolutionary distance, and maximum parsimony methods. Mol Biol Evol 28: 2731–2739

Teske A, Hinrichs KU, Edgcomb V, de Vera Gomez A and others (2002) Microbial diversity of hydrothermal sediments in the Guaymas Basin: evidence for anaerobic methanotrophic communities. Appl Environ Microbiol 68:1994–2007

Tivey MK, McDuff RE (1990) Mineral precipitation in the walls of black smoker chimneys: a quantitative model of transport and chemical reaction. J Geophys Res 95: 12617–12637

Wang F, Zhou H, Meng J, Jiang L and others (2009) GeoChip-based analysis of metabolic diversity of microbial communities at the Juan de Fuca Ridge hydrothermal vent. Proc Natl Acad Sci USA 106:4840–4845

Zhou J, Bruns M, Tiedje J (1996) DNA recovery from soils of diverse composition. Appl Environ Microbiol 62:316–322

Zhou H, Li J, Peng X, Meng J, Wang F, Ai Y (2009) Microbial diversity of a sulfide black smoker in Main Endeavour hydrothermal vent field, Juan de Fuca Ridge. J Microbiol 47:235–247

Zillig W, Reysenbach AL (2001) *Thermococcaceae* fam. nov. In: Boone DR, Castenholz RW (eds) Bergey's manual of systematic bacteriology, Vol. 1 (2nd edn). The *Archaea* and the deeply branching and phototrophic *Bacteria*. Springer, New York, NY, p 341–348

Editorial responsibility: Pei-Yuan Qian, Kowloon, Hong Kong SAR

Submitted: November 7, 2013; Accepted: April 28, 2014
Proofs received from author(s): July 21, 2014